Arabian Journal for Science and Engineering (2019) 44:7033–7046
https://doi.org/10.1007/s13369-019-03768-z

RESEARCH ARTICLE - ELECTRICAL ENGINEERING

Fault Detection During Asymmetrical Power Swing Using Superimposed Negative Sequence Current

Jitendra Kumar[1] · **Premalata Jena**[2]

Received: 16 July 2018 / Accepted: 5 February 2019 / Published online: 18 February 2019

Abstract
Power swing phenomenon occurred during single-pole auto-reclosing (SPAR) period is called asymmetrical power swing. During symmetrical power swing, power swing blocking is used to block distance relay to avoid the selectivity property. Therefore, fault detection is more challenging during asymmetrical power swing since open-pole condition introduces large amount of negative and zero sequence components in voltage and current signals. Further, fault detection during power swing and SPAR prevailed in a series compensated line is more challenging as the metal oxide varistor protecting series capacitor imposes other frequency components. In this paper, a new superimposed negative sequence (NS) current-based technique is proposed to detect the fault incepted in a series compensated line during asymmetrical power swing. The superimposed NS current is calculated using phasor difference between the fault and prefault NS currents. The proposed technique exploits the presence of substantial amount of superimposed NS current during asymmetrical power swing period to detect fault accurately. A summation index is used to declare the fault when it crosses the threshold value. Transient data, obtained from two systems simulated using PSCAD/EMTDC software, are used to test the performance of approach.

Keywords Fault detection · Single-pole tripping (SPT) · Power swing · Series compensation · Superimposed negative sequence current

1 Introduction

Increased power demand, restrictions on building new corridors and new policies have compelled the transmission network to operate close to the stability limit [1]. The acute deficiency in power demand and other limitations can be shorted out by inserting series capacitor in transmission lines [2]. However, the fault incepted in such a line leads to generation of sub-harmonic and super-harmonic components due to the operation of metal oxide varistor (MOV) and series capacitor (SC). Therefore, fault detection is one of the challenging issues for protection engineers [3–8]. Power swing and SPAR are two major stressed conditions which affect the fault detection process in distance relay [9–11]. Line disconnection, loss of large amount of loads, and generator disconnection lead to mismatch in mechanical and electrical powers. As a consequence, slow or fast oscillations are observed in voltage and current signals available at the relay location [9]. During symmetrical power swing, the distance relay remains silent with the help of power swing blocking (PSB) element. However, if a fault occurs during power swing, the operating mode of distance relay is invoked as soon as possible.

SPAR is another stressed situation which also affects the fault detection process in distance relay. In power system, majority of faults are line-to-ground type. To maintain power flow (in other healthy phases), stability, and synchronism between two areas, single-phase tripping and reclosing schemes are maintained instead of three-phase tripping and reclosing [1,11]. However, this situation leads to the presence of substantial amount of negative and zero sequence components in prefault voltage and current signals [9]. The negative and zero sequence based distance relays are maloperated, and it is also observed that these relays are taken out of service from healthy lines of double circuit system. It is essential that the distance relay should detect the fault during power swing and open-pole period prevailed in a series compensated line and generate three-pole tripping signal as

✉ Jitendra Kumar
jeetusingh61@gmail.com

[1] Department of Electrical Engineering, National Institute of Technology Jamshedpur, Jamshedpur, Jharkhand, India

[2] Department of Electrical Engineering, Indian Institute of Technology Roorkee, Roorkee, Uttarakhand, India

quick as possible to maintain stability of the system [11]. However, the distance relay should remain silent for asymmetrical power swing period [9].

Fault detection during power swing present in series compensated lines is mainly discussed in the literature [11–21]. Conventional schemes like rate of change of impedance, concentric circle scheme, and swing center voltage (SCV) are used to discriminate the fault and power swing conditions [11]. In [14], it is described that the time taken by the impedance or apparent resistance trajectory to enter the zones of distance relay decides fault or swing conditions. For fault condition, the trajectory enters the relay zones instantaneously, whereas for power swing, it enters slowly with a time range of 100 ms or more. Hence, a time delay is maintained to discriminate the fault and swing period. However, at certain fault conditions, relay may not operate since it is blocked from operation during power swing period [18]. SCV is another conventional technique which determines the voltage between two sources, and it fails for high resistance and close-in faults [14].

In [12], the phase angle between the fault voltage and current available at relay location is used to identify fault during fast power swing (slip frequency of 5 to 8 Hz). But, this technique has limitation for high resistance faults. The angle of voltage available at relay location is compared with the angles of estimated voltage at the fault point and zone termination voltage [13]. Though this technique overcomes the problem of high resistance fault, its performance is not tested for open-pole period and series compensation cases. In [15], fault detection, classification, and localization techniques are proposed using S-transform and neural network. The major demerit of these techniques is that their performances are not tested for power swing, SPAR, and series compensation cases and moreover the neural network-based technique needs large number of training data set to obtain final output. Another technique based on the time-frequency transform known as S-transform is discussed in [16] to detect the faults during power swing. The technique is dependent on the threshold values and not tested for situations such as SPAR and series compensation.

Technique as mentioned in [17] can detect direction of faults during SPT period using the phase change in fault and prefault NS currents. However, this technique is affected during power swing as the angle oscillates within positive and negative regions. It is not verified for series compensation and high resistance fault cases. In [18,19], Prony and mathematical morphology-based methods are used to extract decaying DC components present in a symmetrical fault current during power swing. The Prony-based technique concentrates on detecting three-phase fault, and it is dependent on fault resistance, location, and inception time of the fault.

In [22], authors have calculated direction of different types of faults incepted in a series compensated line using the phase difference between fault and prefault positive sequence currents. This technique is affected during power swing and load change period. The NS current-based techniques in [23,24] are used to detect the fault incepted in a series compensated line during power swing. However, the technique fails for far-end high resistance fault. Differential power-based technique is proposed in [20] to detect the three-phase fault during power swing. But, this technique is only tested for balanced fault condition. In [21], an adaptive power swing detection criterion based on concentric circle model is developed by considering a ratio of the time required by the swing locus to stay inside the internal circle and the time required by it to pass through the concentric circles. In this work, it is always a tedious work to set the boundary between concentric circles, which depends on the system information. In [25], Teager–Kaiser energy of negative sequence current-based technique is utilized for fault detection during power swing, but it fails during asymmetrical power swing.

This paper aims to provide a solution for fault detection during asymmetrical power swing using superimposed NS current. The superimposed NS component of current is calculated using phasor difference between fault and prefault NS currents. During a symmetrical power swing, the prefault and fault NS currents are substantial in comparison with power swing. Further, the levels of prefault and fault NS currents are increased due to presence of SPAR. The proposed method exploits this feature and uses superimposed NS current to detect the fault. Generally, superimposed technique does not require any reference index. However, this summation index is used to prevent from unintended trip due to varying loading condition during asymmetrical power swing. The technique is independent of voltage information and not affected by voltage distortion. Moreover, the high impedance fault and load change do not affect the proposed scheme.

2 Description of Test System and Analysis of Asymmetrical Power Swing

2.1 System Description

To demonstrate the performance of the proposed technique during asymmetrical power swing, a typical 400 kV, 50 Hz, 9-bus system (as shown in Fig. 1) is considered. In this test system, three generators (600 MVA each) are connected at bus-1, bus-2, and bus-3. System data have been provided in "Appendix" [24]. Relay 'R' located at bus-7 is a test point where fault detection process is to be carried out. The current samples are stored at a sampling frequency of 1 kHz. Further, the phasors of three-phase currents are calculated using discrete Fourier transform (DFT) technique [22]. δ is

power angle between bus-7 and bus-8. Line-78 is 70% series compensated with series capacitor which is placed towards bus-7. Capacitor bank of each phase is protected by MOV. When the fault is close to relay bus, MOV operates as the voltage across the capacitor crosses the threshold value [2]. Capacitor coupling transformer (CVT) and potential transformer (PT) ratios used at this relay location are 400A/5A and 400kV:110V, respectively. The SPAR situation is incepted in line-78 by opening the phase-a poles of B1 and B2, simultaneously following a line-to-ground fault of ag-type (phase-a to ground fault) incepted in it. Further, to generate power swing in the system as provided in Fig. 1, the three poles of B3 and B4 are opened simultaneously following a three-phase fault occurred in line-57. In this process, relay 'R' located at bus-7 experiences asymmetrical power swing. If any fault occurs under such stressed conditions, relay has to detect the fault promptly.

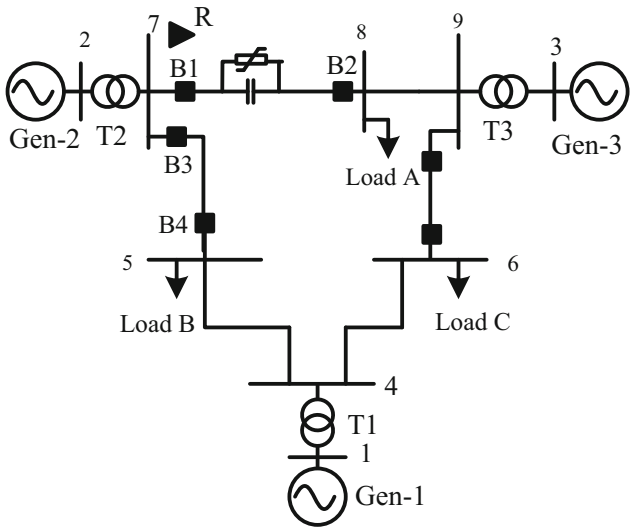

Fig. 1 400 kV, 50 Hz, 9-Bus power system

2.2 Signal Observations During Asymmetrical Power Swing

The current signals measured at relay 'R' during asymmetric power swing (i.e. prefault period) are shown in Fig. 2. For first case, the current samples are collected and sequence currents are calculated at relay location during symmetrical power swing as shown in Fig. 2a. It is evident that there is a presence of small amount of NS current and absence of zero sequence current. Negative sequence current appears because all three phases do not swing, simultaneously. In another case, the current samples are measured during asymmetrical power swing and corresponding calculated sequence currents are shown in Fig. 2b. It is observed from Fig. 2b that the phase-a current of line-78 is zero due to SPAR operation, but at the same time, there is a presence of low-frequency component along with the fundamental frequency component of other healthy phases. This situation leads to the presence of significant amount of negative and zero sequence components along with positive sequence component of current. The presence of substantial amount of NS current during asymmetrical power swing opens an idea to use the superimposed NS current.

When a fault is incepted in a series compensated line, consequently there are variations in other frequency components, swing frequency, and current level which further depend on the compensation level, location of series capacitor, and operation of MOV protecting capacitor bank present in each phase. To test this situation, a three-phase fault is created at 2.8s in line-78 (70% compensated) at a distance of 100 km from the relay location with $\delta = 145°$ without considering SPAR. For such a fault, it is observed from Fig. 3 that the magnitude of fault current is substantially high. As a result, the voltage across the MOV crosses its threshold value and starts conducts. The capacitor is bypassed. As the magnitude of fault current during three-phase fault is increased (shown in Fig. 3a), MOV operates and capacitor is bypassed.

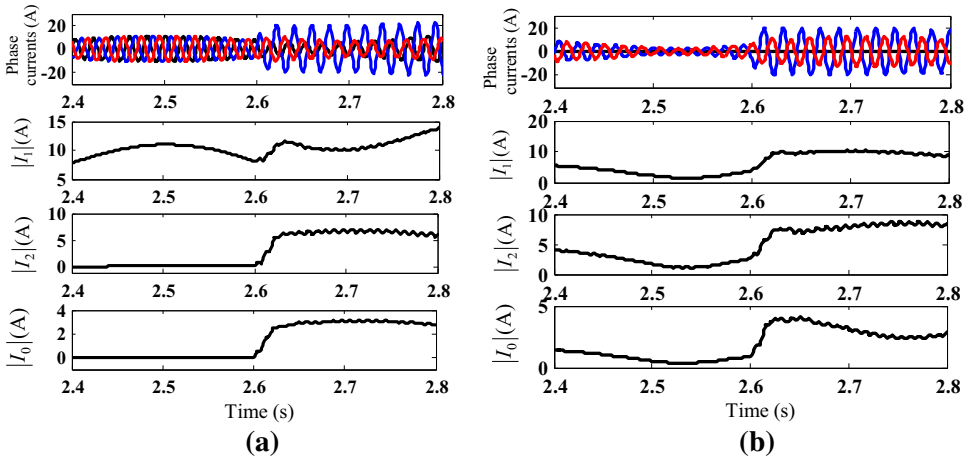

Fig. 2 Prefault phase currents, positive (I_1), negative (I_2), and zero (I_0) sequence currents of line-78 during **a** symmetrical power swing **b** asymmetrical power swing

Hence, the modulation in current signal is present for the initial period (i.e. one cycle) and subsequently, it dies out. Another test case is considered by simulating a bcg-type fault at far-end side (at 260 km from the relay end) with $\delta = 170°$, and it is evident that the current signals (as shown in Fig. 3b) are modulated to a greater extent as compared to previous case (as shown in Fig. 3a). The reason for such a modulation is that MOV doesn't conduct since the voltage across it is within the threshold in case of far-end fault. Another fault case has been simulated during asymmetrical power swing. A bcg-type fault is simulated at a distance of 100 km from the relay location with presence of SPAR in line-78, and the current signals are shown in Fig. 3c. It is observed that the modulation present in current signals is more prominent in comparison with the earlier case (as shown in Fig. 3a). However, in case of bcg-type fault occurred at far end, the current signals (as shown in Fig. 3d) are further distorted and leading to the presence of substantial amount of negative and zero sequence currents.

2.3 Effect of Asymmetrical Power Swing on Distance Relay [26,27]

To analyze the asymmetrical power swing, the relation between three phase electrical output ($P_e = P_{max} \sin\delta$) and rotor angle (δ) can be explained by the swing equation which is defined as

$$\frac{H}{\pi f}\frac{d^2\delta}{dt^2} = P_m - P_{max}\sin\delta \tag{1}$$

where H is the inertia constant and P_m is mechanical input. After consideration of effect of damping winding, the swing equation is modified and provided as

$$\frac{H}{\pi f}\frac{d^2\delta}{dt^2} + D\frac{d\delta}{dt} = P_m - P_{max}\sin\delta \tag{2}$$

where D is damping coefficient.
For disturbance in rotor angle ($\Delta\delta$), the swing equation can be written as

$$\frac{H}{\pi f}\frac{d^2(\delta_0+\Delta\delta)}{dt^2} + D\frac{d(\delta_0+\Delta\delta)}{dt} = P_m - P_{max}\sin(\delta_0+\Delta\delta) \tag{3}$$

With some approximations, electrical power can be written as

$$P_e + \Delta P_e = P_{max}\sin(\delta_0+\Delta\delta) \approx P_{max}\sin\delta_0 + (P_{max}\cos\delta_0)\,\Delta\delta \tag{4}$$

After some approximation, (3) for change in rotor angle can be written as

$$\frac{H}{\pi f}\frac{d^2\Delta\delta}{dt^2} + D\frac{d\Delta\delta}{dt} + P_s\Delta\delta = 0 \tag{5}$$

where P_s is synchronizing power ($P_s = P_{max}\cos\delta_0$).
Initial conditions of (5) are provided in (6).

$$\Delta\delta|_{t=0^+} = \Delta\delta_0 \text{ and } \Delta\dot{\delta}\big|_{t=0^+} = 0 \tag{6}$$

Using (5) and (6), the change in rotor angle [26] can be obtained as

$$\Delta\delta(t) = \frac{\Delta\delta_0}{\sqrt{1-\xi^2}} e^{-\xi\omega_n t}\sin\left(\omega_n t + \cos^{-1}\xi\right) \tag{7}$$

where $\omega_n = (\pi f P_s/H)^{0.5}$,$\xi = D/2(\pi f P_s/H)^{0.5}$
From (4), it is evident that the change in electrical power output is directly proportional to the change in rotor angle. During asymmetrical power swing, three-phase power can be defined as

$$P_{SPAR} = V_b I_b + V_c I_c = V_1 I_1 + V_2 I_2 + V_0 I_0 \tag{8}$$

In Fig. 3, the negative and zero sequence components of electrical power appear with positive sequence component during asymmetrical power swing as expressed in (8). Negative sequence power comes due to unbalancing and zero sequence power comes due to generator grounding. Variation of electrical power is dependent on load variation. It means that asymmetrical power swing appears for long transmission lines where load variation is very high. From (7), initial load angle variation is also the reason of asymmetrical power swing generation. If it is very high, then power swing may be generated due to the SPAR.

For analyzing the behavior of the distance relay during asymmetrical power swing, a power swing (slip frequency of 3.5 Hz) is created in line-78 as shown in Fig. 1. A bg-type fault is initiated in line-78 during an unbalanced power swing at $t = 2.5$ s with fault distance of 100 km and $R_f = 100\,\Omega$. The impedance trajectory enters the trip region of zone-1 at a faster rate and stays there. Hence, relay should detect the fault and generate the trip signal as quick as possible. Impedance trajectory during asymmetrical power swing enters into the trip region of zone 1, zone 2 and zone 3 as shown in Fig. 4a. The impedance trajectory for a bg-type fault incepted in line-78 at a fault distance 100 km and $R_f = 100\ \Omega$ during asymmetrical power swing also enters in mho characteristics which is shown in Fig. 4b.

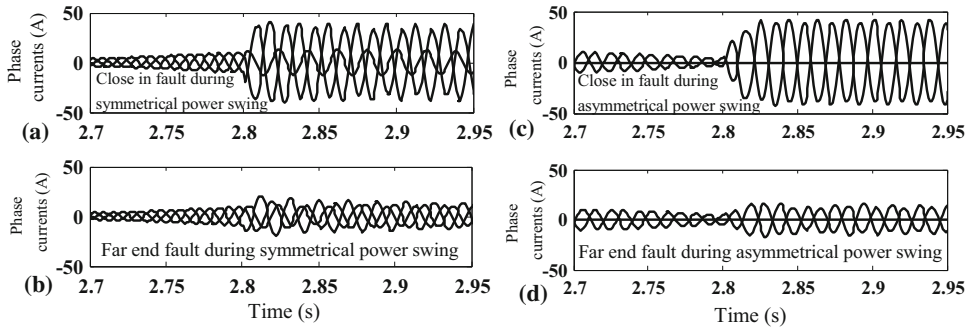

Fig. 3 Phase currents measured at bus-7 for bcg-type fault during symmetrical and asymmetrical power swings with fault distance of **a** 1 km, **b** 100 km, **c** 1 km, **d** 100 km

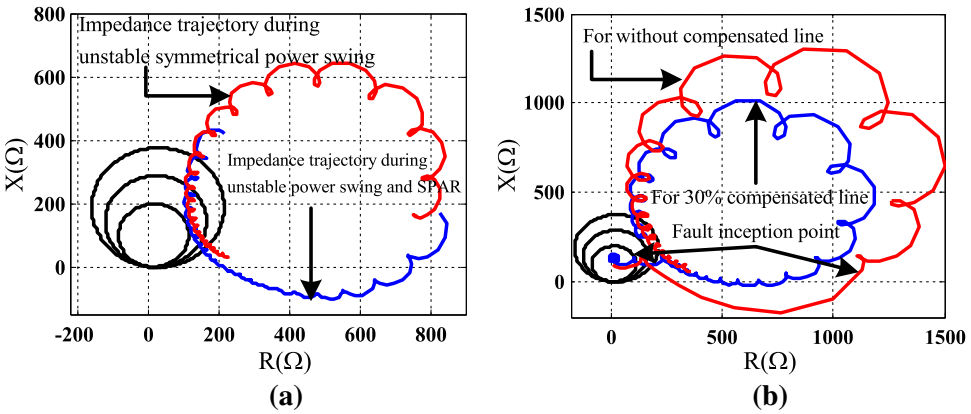

Fig. 4 Impedance trajectories during unstable power swing **a** with and without consideration of SPAR and **b** for line-to-ground fault during SPAR

3 Proposed Fault Detection Scheme During Asymmetrical Power Swing

Fault detection during asymmetrical power swing is challenging task because the modulation in current signal is prevailed due to the operation of MOV and series capacitor. In this paper, superimposed NS current-based technique is proposed to identify the fault incepted in a series compensated line during asymmetrical power swing. The superimposed component of NS current is provided as

$$\left|\Delta \bar{I}_2\right| = \left|\bar{I}_{2\mathrm{F}} - \bar{I}_{2\mathrm{pre}}\right| \tag{9}$$

where $\bar{I}_{2\mathrm{F}}$ and $\bar{I}_{2\mathrm{pre}}$ are the fault and prefault NS currents during stressed system conditions. Further, a summation index g is provided as

$$g_n = \sum_{n=1}^{p} \left[(g_{n-1} + |\Delta I_2|_n - \varepsilon)\right] \tag{10}$$

where g_{n-1} is the previous value of g index and it is initialized with zero, p is total length of samples, and n is the instant of magnitude of NS current. The value of ε depends on the swing frequency rate (slow or fast swing) [28,29]. The index as provided in (10) is used to detect the fault during asymmetrical power swing. This index g is the summation of successive absolute magnitude of superimposed NS current. When the index exceeds threshold value (h), the fault is registered by the relay.

A fault detection criterion can be provided as

$$g(n) > h \tag{11}$$

If $g(n)$ increases above the threshold 'h', then fault is detected and a trip signal is generated. 'h' is selected on the basis of the prefault values of superimposed NS current generated during different fault situations. A rigorous simulation study is required to decide the threshold value. For taking the decision of threshold value, more than 200 fault cases are simulated for different system conditions such as low loading and various compensation levels. From extensive simulation study, it is observed that the maximum prefault fault value of NS current is below of 0.0001. Therefore, value of threshold is kept 0.001 with extra precautions to improve selectivity property of the algorithm.

Flowchart for the execution of the proposed algorithm is shown in Fig. 5. Initially, the prefault and fault three-phase currents are sampled at a sampling frequency of 1 kHz. The phasors of three-phase current signals are calculated using DFT technique.

Thereafter, the NS component of fault and prefault currents are calculated. Further, the superimposed NS current is estimated using the expression as provided in (9). Finally, the index 'g' is calculated using (10) and component with the threshold value 'h'. If the value of index 'g' crosses the

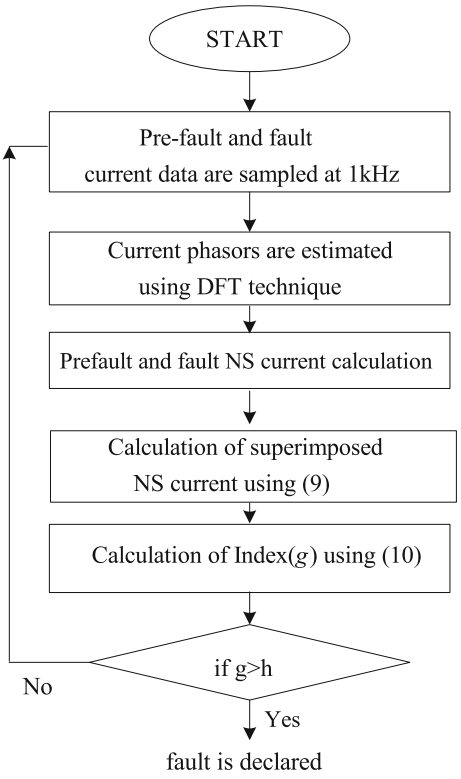

Fig. 5 Flowchart for execution of the proposed algorithm

threshold, then fault is declared for further action at relay end.

4 Performance Evaluation of Proposed Technique

To test the performance of the proposed algorithm for different types of faults during asymmetrical power swing, transient data are generated from the system (shown in Fig. 1) which is simulated using PSCAD/EMTDC software and used for further NS component calculation. Throughout the simulation process, the nonlinear models of current transformer (CT with Lucas model) and capacitor coupling voltage transformer (CCVT) are considered. To calculate the superimposed component of NS currents, 10 cycles of prefault current signals are stored in relay memory. Different fault cases are simulated and described one by one in the following subsections to validate the performance of the proposed approach.

4.1 Line-to-Ground Fault for Very High Fault Resistance

To test the performance of the proposed scheme, a bg-type fault with fault resistance (R_f) $= 400\ \Omega$ is incepted in line-78

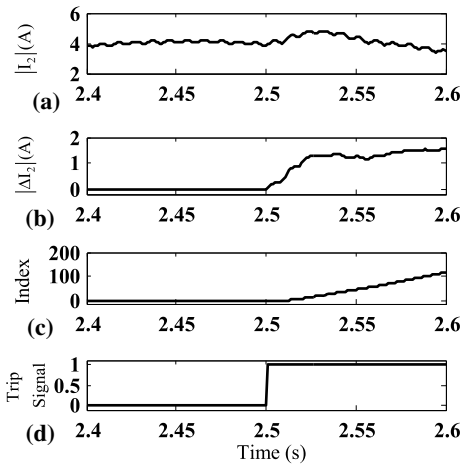

Fig. 6 Results for bg-type of very high resistance fault ($R_f = 400\ \Omega$) during asymmetrical power swing. **a** $|I_2|$, **b** $|\Delta I_2|$, **c** Index, 'g', **d** Trip signal

with $\delta = 170°$ and slip frequency of 3.5 Hz during asymmetrical power swing. The performance plot for this case is shown in Fig. 6. It is evident from figure that the magnitude of NS fault current is very less. In this case, level of fault current does not affect the performance of the proposed technique since the magnitude of the superimposed component is increasing after fault inception point. Finally, the magnitude of index 'g' is growing in positive direction and corresponding output is '1', which perfectly declares the fault condition.

4.2 Far-End Single Line-to-Ground Fault

For far-end fault, the fault path impedance is large and current magnitude decreases considerably in comparison with the prefault load current. To evaluate the output of the proposed approach, a bg-type fault is created at $t = 2.5$ s for 250 km away from relay end with $R_f = 100\ \Omega$.
The magnitude of NS current is considerably less for far-end fault case but the level of superimposed NS current is sufficient to detect the fault. The rise of summation index as shown in Fig. 7 provides the indication of fault during asymmetrical power swing.

4.3 Close-in Fault

Proposed technique is based only on current information, and it is free from the voltage transient issues. Moreover, location of CCVT (line side or bus side) also does not affect the performance of the technique as it is free of voltage information. For series compensated line, fault just after capacitor bank leads towards voltage and current inversion situations, which further add other frequency components in fundamental signals. To test such scenario, a bg-type fault is created at

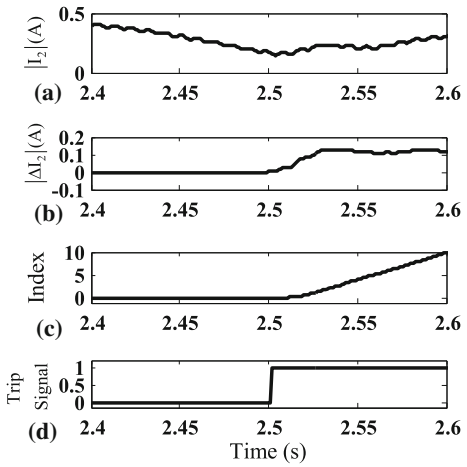

Fig. 7 Results for far-end bg-type fault (fault distance=250 km) during asymmetrical power swing. **a** $|I_2|$, **b** $|\Delta I_2|$, **c** Index, 'g', **d** Trip signal

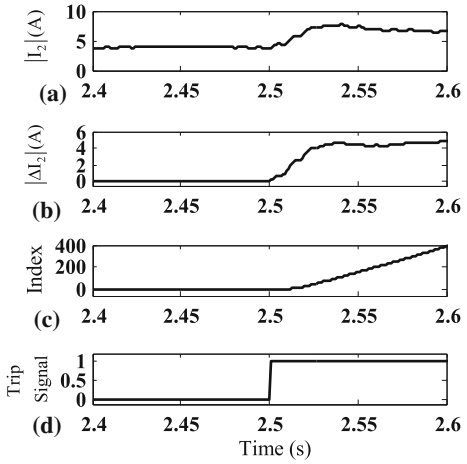

Fig. 8 Results for close-in bg-type fault (fault distance=1 km) during asymmetrical power swing. **a** $|I_2|$, **b** $|\Delta I_2|$, **c** Index, 'g', **d** Trip signal

1 km from relay bus with $R_f = 100\,\Omega$ during asymmetrical power swing ($\delta = 120°$). During this condition, superimposed NS current appears from prefault to fault period as shown in Fig. 8. The rise in magnitude of 'g' clearly indicates the presence of fault and corresponding trip signal is at '1' consistently.

4.4 Experimental Results with Real-Time Digital Simulator (RTDS)

The proposed technique is also tested on real-time platform using real-time digital simulator (RTDS) procured from RTDS Technologies Inc., Winnipeg, Canada. For such purpose, 9-bus system as shown in Fig. 1 is developed using the RSCAD software available in RTDS. The RTDS platform as shown in Fig. 9 comprises PB5 processor boards with a workstation interfaced with various other auxiliary components. It

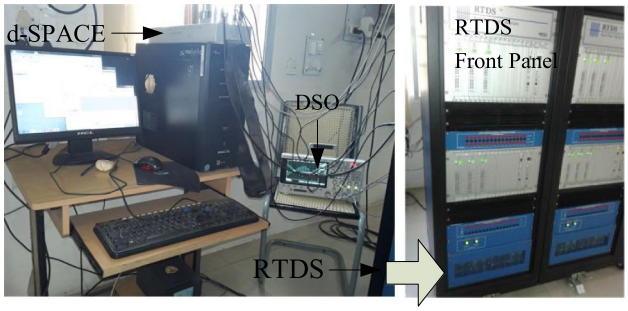

Fig. 9 Experimental setup

has an inbuilt RSCAD software package for performing the necessary fault detection, classification and location process.

The necessary hardware-in-the loop (HIL) test bed using real-time simulator and dSPACE are shown in Fig. 9. The proposed algorithm for fault detection during asymmetrical power swing is developed in MATLAB/Simulink. The algorithm steps developed in Simulink environment are converted into a C code and transferred to the dSPACE-401 processor by means of Control Desk software. The processor has its own Analog/Digital (A/D) and Digital /Analog (D/A) ports with an input and output range of ± 10 V to communicate with RTDS. Real-time three-phase current signals available at relay 'R' are delivered from the output port of GPC card through Giga Transceiver Analogue Output (GTAO) card to the processor (dSPACE-401) where the proposed algorithm is present. It is to be noted that current signals available at the output port of RTDS are scaled to the range of 10 V. The algorithm embedded in the processor of the controller is executed, and trip signal is generated in the form as output. To demonstrate such a process, a cg-type fault is created in line-78 at 60 km from relay 'R' location with $R_f = 15\ \Omega$ during asymmetrical power swing. The three-phase current signals are sent to dSPACE through GTAO card. After execution of the algorithm in dSPACE, the corresponding trip signal is generated and it is captured by DSO-X2014 which is shown in Fig. 10a, b. It is observed that the trip signal status is '1' from the fault inception point onwards. For cg-type fault, corresponding simulated results for three-phase current, NS current, superimposed NS current, index, and trip signal are shown in Fig. 10c–g, respectively.

In the similar way, a bcg-type fault is incepted in the same line during asymmetrical power swing. Corresponding experimental results are shown in Fig. 11a, b. It is observed that the superimposed NS current is significant after the fault inception point and the trip signal is generated promptly to declare the fault accurately. To verify experimental results, the same bcg-type fault is simulated using the EMTDC/PSCAD software and the corresponding results are shown in Fig. 11c–g. By comparing both the results obtained from hardware and simulation platform, it is found that the

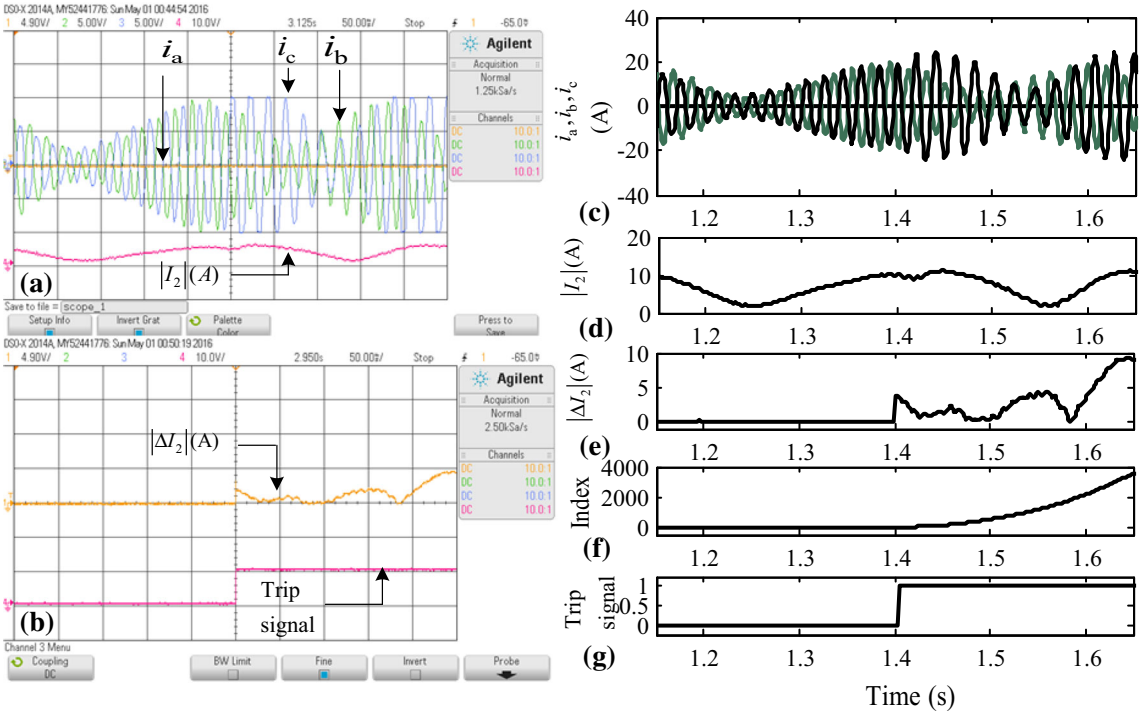

Fig. 10 Dynamic performance plots (experimental and simulated) of the proposed technique for cg-type fault. **a** Experimental three-phase currents and $|I_2|$, **b** $|\Delta I_2|$ and trip signal, **c** Simulated three phase currents, **d** $|I_2|$, **e** $|\Delta I_2|$, **f** Index, **g** Trip signal

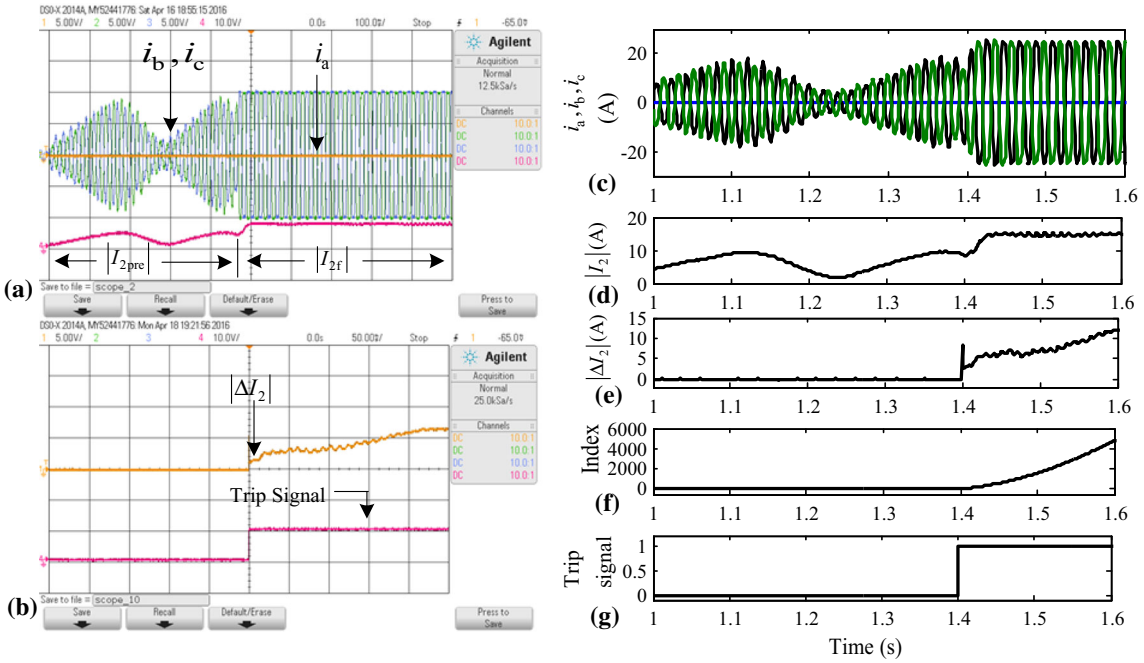

Fig. 11 Dynamic performance plots (experimental and simulated) for the proposed technique for bcg-type fault incepted in line-78. **a** Experimental three-phase currents and $|I_2|$, **b** $|\Delta I_2|$ and trip signal, **c** Simulated three-phase currents, **d** $|I_2|$, **e** $|\Delta I_2|$, **f** Index, **g** Trip signal

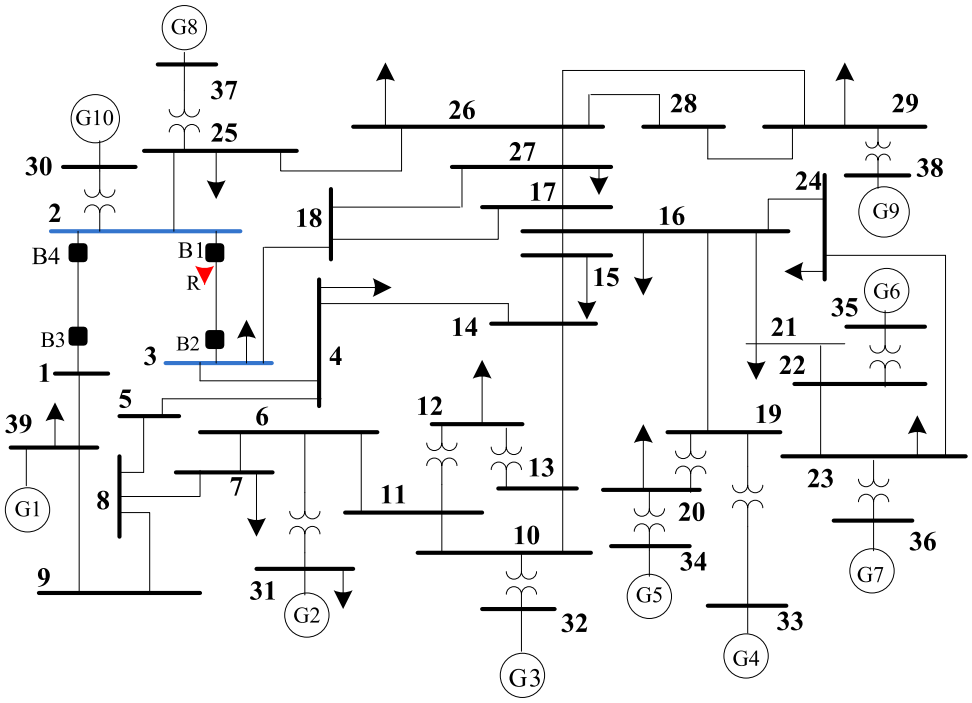

Fig. 12 Typical 39-bus system

superimposed NS current pattern is almost same and trip signal generation time matches with each other.

5 Performance Evaluation of Proposed Scheme for New England 39-Bus System

To evaluate the performance of the proposed algorithm, New England 10-machine, 39-bus system as shown in Fig. 12 is considered. Line-23 is 60% series compensated. Relay 'R' located at bus-2 protects line-23 and considered as the test point where the fault detection is to be carried out. SPAR is initiated in line-23 by opening corresponding phase-a poles of breakers (i.e. B1 and B2) present at both sides of the line following an ag-type fault incepted in it. During SPAR period, a three-phase fault is created in line-12 and cleared by opening the breakers (i.e. B3 and B4) present at both sides simultaneously. As a result, power swing is experienced in voltage and current signals available at relay 'R' located at bus-2. Here, the slip frequency is found to be 2.8 Hz. To verify the performance of the proposed approach, two fault cases are simulated and results are discussed in following subsections.

5.1 Performance of Proposed Scheme During Far-End High Resistance Fault

The performance of the proposed technique is tested for a bcg-type fault by creating in the line-23 at $t = 3.5$ s for a fault distance of 240 km with a fault resistance of 200 Ω

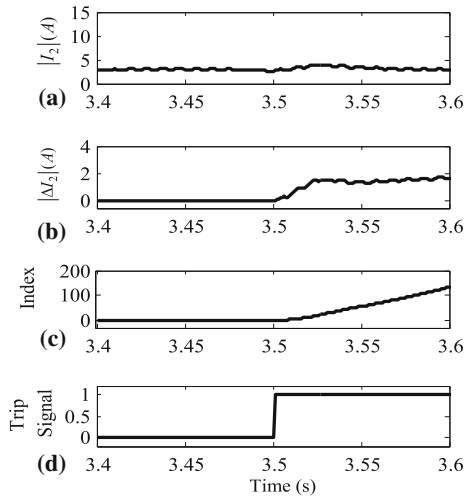

Fig. 13 Performance of the proposed scheme for bcg-type fault incepted in line-23 (fault distance 240 km, $R_f = 200\,\Omega$). **a** $|I_2|$, **b** $|\Delta I_2|$, **c** Index, **d** Trip signal

($\delta = 150°$). For such a fault, the level of fault current is considerably less. In such a case, there is a less possibility of conduction of MOV as voltage across capacitor bank is below of it's threshold. It is observed that sub-synchronous oscillation is more prominent for far-end fault case as MOV conduction is negligible and capacitor bank conducts the entire fault current [2]. However, the magnitudes of superimposed NS current and index as shown in Fig. 13b, c are sufficient to declare the fault under such fault case.

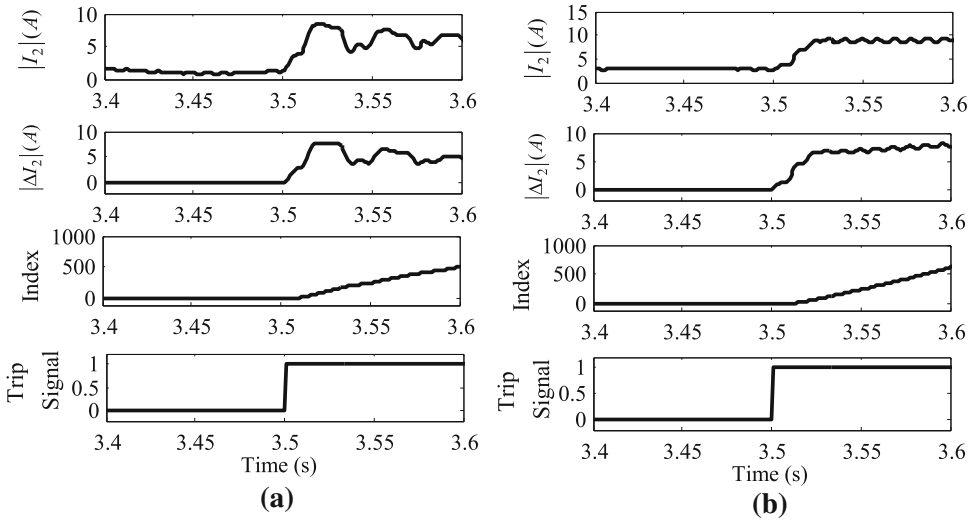

Fig. 14 $|I_2|$, $|\Delta I_2|$, Index of proposed scheme, trip signal for bc-type fault incepted in line-23 (fault distance 150 km, $R_f = 5\,\Omega$) for different compensation levels. **a** 20% and **b** 60%

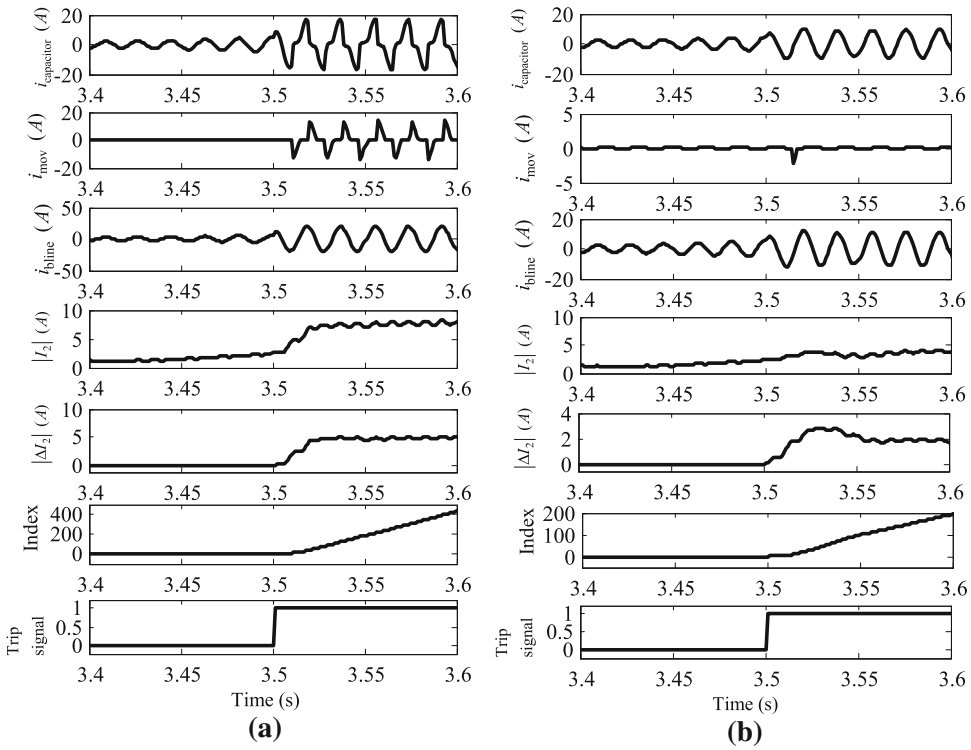

Fig. 15 Capacitor current ($i_{capacitor}$), MOV current (i_{mov}), Line current (i_{bline}), $|I_2|$, $|\Delta I_2|$, Index, and Trip signal for bg-type fault incepted at line-23 for different fault distances. **a** 7 km, **b** 200 km

5.2 Effect of Different Compensation Level (20% and 60%)

To check the effect of compensation levels (20% and 60%) on the proposed approach, a bc-type fault is incepted in line-23 at a distance of 150 km at $t = 3.4$ s with 20% compensation under asymmetrical power swing. Corresponding results are shown in Fig. 14a. It could be observed that the consistent growth of the index in positive direction helps in detecting the fault correctly.

The similar type of fault is created under similar situation with 60% of compensation level. The corresponding results are shown in Fig. 14b. The results obtained for such a fault scenario are correct as the superimposed NS current is prominent throughout the fault period, and the index has crossed the limit well above the threshold. It is observed from various simulation studies that the voltage and current signals available at relay end oscillate less for higher compensation level during without SPAR situation. On the other hand, the presence of SPAR in a series compensated line with higher compensation level leads towards a more unbalancing situation.

5.3 Effect of MOV Operation for Different Fault Distance

In series compensated line, MOV is used to provide overvoltage protection for the capacitor bank present in each phase. In normal conditions, MOV doesn't conduct and the line current is equal to the current flowing through the capacitor bank. However, in case of close-in fault, the voltage across series capacitor increases above the threshold value and MOV operates. To analyze the effect of MOV operation, a bg-type fault is incepted in line-23 at 3.5 s with $R_f = 0.01\ \Omega$ at a distance of 7 km from relay location during asymmetrical power swing. During this fault period, the line current (i_{bline}) is the resultant of currents through MOV (i_{mov}) and capacitor bank ($i_{capacitor}$). It is observed that the values of superimposed NS current and index 'g' are above the threshold and declaring the fault correctly, even during MOV operation. The performance of the proposed approach for such fault scenario is shown in Fig. 15a.

The analysis is concentrated on far-end fault situation and MOV operation. To demonstrate the performance of the proposed technique for this situation, a bg-type fault is created at 200 km fault distance with $R_f = 0.01$ at 3.5 s. The corresponding performance plot is shown in Fig. 15b. It is observed that magnitude of the fault current is considerably less in comparison with that of close-in bg-type fault as shown in Fig. 15a. However, the magnitude of the superimposed NS current is well above the desired value. Index grows in a positive direction which is the indication of fault.

6 Comparative Study of Proposed Scheme

In this section, the comparative assessment of proposed technique with several conventional techniques is carried out. Many research papers are available for detecting the fault during symmetrical power swing for uncompensated lines. Sample-to-sample and cycle-to-cycle comparison schemes are not able to detect the fault during power swing due to modulation in current and voltage signals. The conventional techniques based on rate of change of apparent resistance, swing center voltage (SCV), and superimposed positive sequence current are considered for the comparative assessment with the proposed scheme. To compare the performances of these techniques with proposed approach, a bg-type fault is created at 2.5 s in line-78 (70% compensated) of Fig. 1 at a distance of 100 km from relay location with a slip frequency of 3.5 Hz, $\delta = 170°$. The dynamic plots of each of the conventional techniques (rate of change of R, rate of change of SCV and superimposed positive sequence current) and proposed method are shown in Fig. 16. It is observed that the values of R and SCV are zero throughout the fault period and their values remain high before the

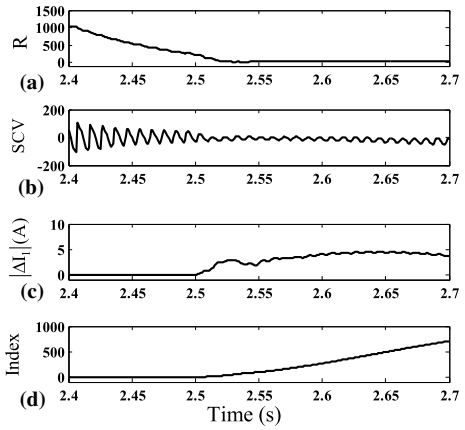

Fig. 16 Comparative assessment of the conventional techniques with proposed approach during asymmetrical power swing for bg-type fault with $R_f = 100\ \Omega$. **a** R seen by the relay, **b** SCV, **c** $|\Delta I_1|$, **d** Index g

fault inception point. This situation leads towards a conflict in deciding the threshold value. Though the superimposed positive sequence current based technique operates correctly, but it operates wrongly for load change case. For such a fault case, performance plot of the proposed approach is shown in Fig. 16d. It is clear from the figure that proposed technique works well and detects the fault within 3 ms.

The performances of other three conventional techniques [18,19] are discussed for comparing with proposed approach. In [18], it is described that the presence of decaying DC component of any phase current is the indication of symmetrical fault during power swing. However, the presence of decaying DC components for far-end high resistance line-to-ground fault during power swing present in a series compensated line could not be detected as the magnitude of DC component during fault period is almost equal with the prefault components. For testing purpose, a bg-type fault is created at 2.5 s with a distance of 270 km with 200 Ω during asymmetrical power swing for 20% series compensated line. For such a fault case, decaying DC of phase-b current is shown in Fig. 17a. It is clear that the amplitudes of decaying DC components are almost equal with the prefault values and therefore it is difficult to maintain threshold. Absence of decaying DC component during high resistance far-end fault creates problem in deciding the threshold to differentiate prefault and fault condition. During prefault case, some amount of decaying dc appears due to fast modulation of voltage and current signals. However, for the same fault situation, the fault can be detected by proposed approach correctly as the index grows from the fault point onwards (Fig. 17d).

In [24], cumulative sum (CUSUM) of NS current-based scheme is utilized for fault detection during power swing. To evaluate the relative analysis, a bg-type fault (fault distance 250 km, $R_f = 250\ \Omega$) is initiated at 2.5 s during asymmetrical power swing for 20% series compensated line.

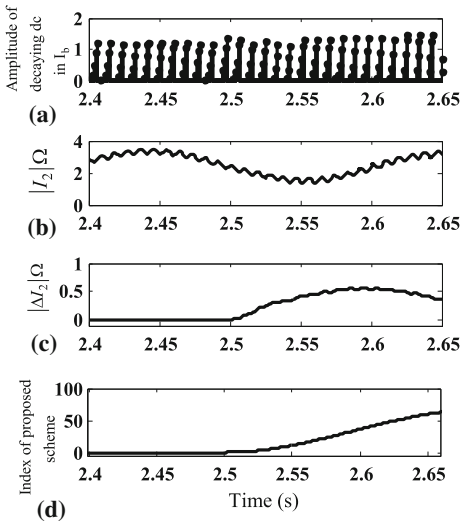

Fig. 17 Comparison of the proposed scheme with existing scheme provided in [18] for 20% series compensated line for bg-type fault created at 270 km with $R_f = 200\,\Omega$. **a** $|I_2|$, **b** $|\Delta I_2|$, **c** Index, 'g', **d** Trip signal

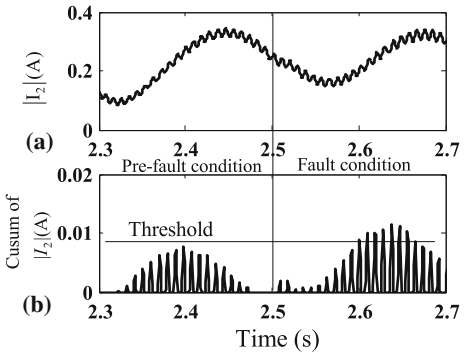

Fig. 18 Comparison of proposed scheme with the scheme described in [24] for 20% series compensated line for bg-type fault created at 250 km with $R_f = 250\,\Omega$. **a** $|I_2|$, **b** CUSUM of $|I_2|$

It is observed from Fig. 18 that the value of CUSUM of I_2 is less after fault inception point, but its value is large during prefault condition. This creates the conflict in deciding the threshold value. For similar condition, performance of proposed scheme is shown in Fig. 19. It is observed from Fig. 19 that proposed technique works for such a scenario correctly. The superiority of the proposed method with respect to CUSUM method is mentioned as the lack of necessity to define a threshold.

The main advantage of the proposed scheme is to provide the solution for fault detection during asymmetrical power swing. Proposed scheme has been tested for different compensation levels and different types of fault conditions, and it is found that it performs well in all system conditions. Proposed scheme takes very less time (approximately 3 ms–5 ms) due to use of local end data. The variation of negative sequence current from prefault to fault condition makes the proposed scheme more useful for different fault

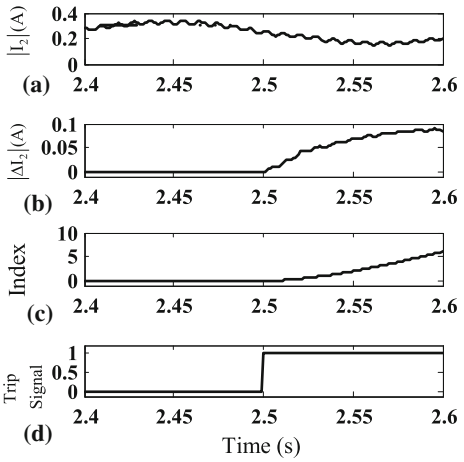

Fig. 19 Performance of proposed scheme for 20% series compensated line when bg-type fault is created at 250 km with $R_f = 250\,\Omega$. **a** $|I_2|$, **b** $|\Delta I_2|$, **c** Index of proposed scheme, **d** Trip signal

cases. This scheme is only dependent on the current information; therefore it is free from the CCVT transients or any variation occurred in voltage. Negative sequence current is independent of system loading variations; therefore, for superimposed negative sequence currents-based technique provides the fault detection solution for varying loading conditions also.

7 Conclusion

Power swing and SPT are two stressed system conditions in power network. Fault detection during such conditions for a series compensated line remains one challenging task. In this paper, superimposed NS current-based technique is proposed for the fault detection during aforementioned conditions for series compensated line. Initially, SPT is created in a particular line and after onwards power swing is created in the same line. This technique uses the stored samples of prefault current at the relay location. A change in summation of NS superimposed component is utilized for the fault detection. The proposed approach is almost independent of threshold value as the superimposed current values before fault is approximately zero. However, the threshold is maintained for a situation where the signal is having noise. This scheme works well for different types of faults like close-in fault, high resistance fault, single line-to-ground fault, double line-to-ground fault, line-to-line fault, far-end fault for different compensation levels, fault locations, power angle, slip frequencies and fault resistances. This scheme utilizes the magnitude of superimposed current, and it is immune to voltage–current inversion. It is not affected from CCVT transients in case of close-in fault as it is independent of voltage information. Proposed scheme is also tested

on 9-bus and 39-bus system using RSCAD/RTDS. The comparative assessment is also analyzed with different schemes. It is found that proposed scheme provides accurate and fast results.

Appendix

System data
Load-A=300 MW, 100 MVAr., Load-B=200 MW, 75 MVAr., Load-C=150 MW, 75 MVAr.
Generators:
Generator-1: 600 MVA, 22 kV, 50 Hz, 4.4 MW/MVA
Generator-2: 465 MVA, 22 kV, 50 Hz, 4.4 MW/MVA
Generator-3: 310 MVA, 22 kV, 50 Hz, 4.4 MW/MVA
Common parameters of generators:
$X_{\mathrm{d}} = 1.81\,\mathrm{p.u.}$, $X'_{\mathrm{d}} = 0.3\,\mathrm{p.u.}$, $X''_{\mathrm{d}} = 0.23\,\mathrm{p.u.}$, $T'_{\mathrm{d0}} = 8\,\mathrm{s}$, $T''_{\mathrm{d0}} = 0.03\,\mathrm{s}$, $X_q = 1.76\,\mathrm{p.u.}$, $X''_{\mathrm{q}} = 1.76\,\mathrm{p.u.}$, $T''_{\mathrm{q0}} = 0.03\,\mathrm{s}$,
Potier reactance (X_{p})=0.15 p.u.
Transformers:
T1: 600 MVA, 22 kV/400 kV, 50 Hz, Delta/Grounded Star, $X = 0.163\,\mathrm{p.u.}$
T2: 465 MVA, 22 kV/400 kV, 50Hz, Delta/Grounded Star, $X = 0.163\,\mathrm{p.u.}$
T3: 310 MVA, 22 kV/400 kV, 50 Hz, Delta/Grounded Star, $X = 0.163\,\mathrm{p.u.}$
Common parameters of Transformers:
$X_{\mathrm{core}} = 0.33\,\mathrm{p.u.}$, Copper losses = 0.00177 p.u.
Transmission line:
Length of line-78 = 320 km., line-89 = 400 km., line-75 = 310 km., line-54 = 350 km, line-64 = 350 km.,
Line-69 = 300 km.
Data of each line:
Positive sequence impedance $= 0.12 + j0.88\Omega/\mathrm{km}$
Positive sequence capacitive reactance $= 0.487\,\mathrm{M\Omega km}$
Zero sequence impedance resistance $= 0.309 + j1.297\ \Omega/\mathrm{km}$
Zero sequence capacitive reactance $= 0.41934\,\mathrm{M\Omega km}$

References

1. Power System Relay Committee: Power swing and out of step considerations on transmission lines. In: IEEE PSRC WG D6, pp. 1–59. http://www.pes-psrc.org/Reports/Power%20Swing%20and%20OOS%20Considerations%20on%20Transmission%20Lines%20F.pdf (2005)
2. Kasztenny, B.: Distance protection of series-compensated lines: problems and solutions. In: 28th Annual western protective relay conference (GER-3998), pp. 1–34. http://store.gedigitalenergy.com/FAQ/Documents/Alps/GER-3998.pdf (2001)
3. Coursol, M.; Nguyen, C.T.; Lord, R.; Do, X.D.: Modeling MOV-protected series capacitors for short-circuit studies. IEEE Trans. Power Deliv. **8**(1), 448–453 (1993)
4. Goldsworthy, D.L.: A linear model for MOV-protected series capacitors. IEEE Trans. Power Syst. **PWRS–2**(4), 953–957 (1987)
5. Lucas, P.G.; Mclaren, J.R.: A computationally efficient MOV model for series compensation studies. IEEE Trans. Power Deliv. **6**(4), 1491–1497 (1991)
6. Mahseredjian, J.: Superposition technique for MOV-protected series capacitors in short-circuit calculations. IEEE Trans. Energy Convers. **10**(3), 1394–1400 (1995)
7. Abdelaziz, A.Y.; Mekhamer, S.F.; Ezzat, M.: Fault location of uncompensated/series-compensated lines using two-end synchronized measurements. Electr. Power Compon. Syst. **41**(7), 693–715 (2013)
8. Biswal, M.; Pati, B.B.; Pradhan, A.K.: Directional relaying of series-compensated line using an integrated approach. Electr. Power Compon. Syst. **40**(7), 691–710 (2011)
9. Calero, F.; Hou, D.: Practical considerations for single-pole-trip line-protection schemes. In: Engineers 2005 58th annual conference, pp. 1–31. https://www.selinc.com/WorkArea/DownloadAsset.aspx?id=3670 (2005)
10. Moaddabi, N.; Hosseinian, S.H.; Gharehpetian, G.B.: Practical framework for self-healing of smart grids in stable/unstable power swing conditions. Electr. Power Compon. Syst. **40**(6), 575–596 (2012)
11. Mooney, J.P.E.; Fischer, N.: Application guidelines for power swing detection on transmission systems. In: 59th Annual conference for protective relay engineers, pp. 289–298 (2006)
12. Machraoui, A.; Thomas, D.W.P.: A new blocking principle with phase and earth fault protection during fast power swings for distance protection. IEEE Trans. Power Deliv. **10**(3), 1242–1248 (1995)
13. Machraoui, A.; Thomas, D.W.P.: A new principle for high resistance earth fault detection during fast power swings for distance protection. IEEE Trans. Power Deliv. **12**(4), 1452–1457 (1997)
14. Benmouyal, G.; Hou, D.; Tziouvaras, D.: Zero-setting power-swing blocking protection. In: 31st Annual western protective relay conference, Spokane, Washington, pp. 1–32 (2004)
15. Roya, N.; Bhattacharya, K.: Detection, classification, and estimation of fault location on an overhead transmission line using S-transform and neural network. Electr. Power Compon. Syst. **43**(4), 461–472 (2015)
16. Samantaray, S.R.; Dubey, R.K.; Chitti Babu, B.: A novel time–frequency transform based spectral energy function for fault detection during power swing. Electr. Power Compon. Syst. **40**(8), 881–897 (2012)
17. Jena, P.; Pradhan, A.: Directional relaying during single-pole tripping using phase change in negative-sequence current. IEEE Trans. Power Deliv. **28**(3), 1548–1557 (2013)
18. Lotfifard, S.; Faiz, J.; Kezunovic, M.: Detection of symmetrical faults by distance relays during power swings. IEEE Trans. Power Deliv. **25**(1), 81–87 (2010)
19. Morais, A.P.; Junior, G.C.; Moriotto, L.; Marchesan, G.: A morphological filtering algorithm for fault detection in transmission lines during power swings. Electr. Power Syst. Res. **122**, 10–18 (2015)
20. Rao, J.G.; Pradhan, A.K.: Differential power-based symmetrical fault detection during power swing. IEEE Trans. Power Deliv. **27**(3), 1557–1564 (2012)
21. Lin, X.; Li, Z.; Ke, S.; Gao, Y.: Theoretical fundamentals and implementation of novel self-adaptive distance protection resistant to power swings. IEEE Trans. Power Deliv. **25**(3), 1372–1383 (2010)
22. Jena, P.; Pradhan, A.: A positive-sequence directional relaying algorithm for series-compensated line. IEEE Trans. Power Deliv. **25**(4), 2288–2298 (2010)
23. Nayak, P.K.; Pradhan, A.K.; Bajpai, P.: Detecting fault during power swing for a series compensated line. In: 2011 IEEE interna-

tional conference on energy, automation and signal (ICEAS), pp. 1–69 (2011)
24. Nayak, P.K.; Pradhan, A.K.; Bajpai, P.: A fault detection technique for the series compensated line during power swing. IEEE Trans. Power Deliv. **28**(2), 714–722 (2013)
25. Kumar, J.; Jena, P.: Solution to fault detection during power swing using Teager–Kaiser energy operator. Arab. J. Sci. Eng. **42**(12), 5003–5013 (2017)
26. Hashemi, S.M.; Sanaye-Pasand, M.: Distance protection during asymmetrical power swings: challenges and solutions. IEEE Trans. Power Deliv. **PP**(99), 1 (2018)
27. Jena, P.; Pradhan, A.: Directional relaying during power swing and single-pole tripping. In: IEEE third international conference on power systems, Kharagpur, India (2009)
28. Nayak, P.K.; Pradhan, A.K.; Bajpai, P.: Secured zone 3 protection during stressed condition. IEEE Trans. Power Deliv. **30**(1), 89–96 (2015)
29. Kumar, J.; P. Jena, P.: Detection of fault during power swing using superimposed negative sequence apparent power based scheme. In: CERA-2017, IIT Roorkee, India (2017)
30. Moravej, Z.; Pazoki, M.; Khederzadeh, M.: Impact of UPFC on power swing characteristic and distance relay behavior. IEEE Trans. Power Deliv. **29**(1), 261–268 (2014)